Supplementary material

Extended kinetic method and RRKM modeling to reinvestigate proline's proton affinity and approach the meaning of effective temperature.

Denis Lesage,[1*] Sakina Mezzache,[1] Yves Gimbert,[1,2] Héloïse Dossmann,[1] Jean-Claude Tabet[1,3].

[1] Sorbonne Université, CNRS, Institut Parisien de Chimie Moléculaire, IPCM, 75005 Paris, France. Email: denis.lesage@sorbonne-universite.fr

[2] Univ. Grenoble Alpes and CNRS, DCM (UMR 5250) BP 53, 38041 Grenoble Cedex 9, France.

[3] Service de Pharmacologie et d'Immunoanalyse (SPI), Laboratoire d'Etude du Métabolisme des Médicaments, CEA, INRA, Université Paris Saclay, MetaboHUB, F-91191 Gif-sur-Yvette, France.

Table S1. PA values of amines used as reference bases.[a]

Amines (B_i)	$PA(B_i)$ ($kJ.mol^{-1}$)
(1) Pyridine	930.0
(2) Cyclohexylamine	934.4
(3) 3-Picoline	943.4
(4) 4-Vinylpyridine	944.1
(5) 4-Picoline	947.2
(6) Pyrrolidine	948.3

[a] All values taken from Hunter EP, Lias SG. Evaluated Gas Phase Basicities and Proton Affinities of Molecules: An update. *J. Phys. Chem. Ref. Data*. 1998; 27: 413.

Table S2. Energetics data (Hartrees) relative to the proline and prolineH$^+$ obtained at the G4 level of theory.

	G4(0K)[a]	G4 Energy[b]
Proline	-400.945746	-400.938451
ProlineH$^+$	-401.294598	-401.302061

[a] Zero-point-corrected electronic energy (0 K)
[b] Thermal-corrected energy (298.15 K)

Table S3. Cartesian coordinates of all compounds involved in this work.

	x	y	z
Proline			
N	0.722033	-1.039518	0.556478
C	1.99912	-0.633939	-0.072573
C	-0.129836	0.159528	0.751246
H	2.361814	-1.416932	-0.745204
H	2.779536	-0.448855	0.679602
C	1.645293	0.669031	-0.79701
C	0.681859	1.347226	0.189534
H	-0.385708	0.315379	1.803772
C	-1.470369	-0.012679	0.002894
H	1.13359	0.448224	-1.740198
H	2.526227	1.272035	-1.02644
H	0.031318	2.097586	-0.26124
H	1.245753	1.827107	0.995917
O	-1.588882	-1.19276	-0.612357
O	-2.316479	0.842208	-0.018205
H	0.868852	-1.546905	1.419313
H	-0.729121	-1.6416	-0.420915
ProlineH^+			
N	0.788292	-1.031707	0.57435
C	2.069386	-0.554686	-0.098533
C	-0.13303	0.165606	0.760279
H	2.438663	-1.347694	-0.748652
H	2.79668	-0.364861	0.69298
C	1.638583	0.729581	-0.802635
C	0.657083	1.366957	0.195198
H	-0.387526	0.276474	1.815167
C	-1.394087	-0.184628	-0.036511
H	1.145016	0.499668	-1.75201
H	2.494293	1.37056	-1.017805
H	-0.011995	2.098709	-0.257906
H	1.194399	1.863231	1.007309
O	-1.476012	-1.2069	-0.675937
O	-2.315971	0.753897	0.07279
H	0.973659	-1.523035	1.448666
H	-3.100823	0.502501	-0.443387
H	0.247846	-1.666566	-0.046423

Detailed example of application

For the [Pro H^+ Pyr] heterodimer, the "concentration" of the precursor ion (first normalized to 1) and the concentration of the two competitive $ProH^+$ and $PyrH^+$ product ions, calculated at different points of the mass spectrometer using *MassKinetics* software, are reported in Fig. S1(a). The corresponding internal energy distributions of the precursor ion are shown in Fig. S1(b).

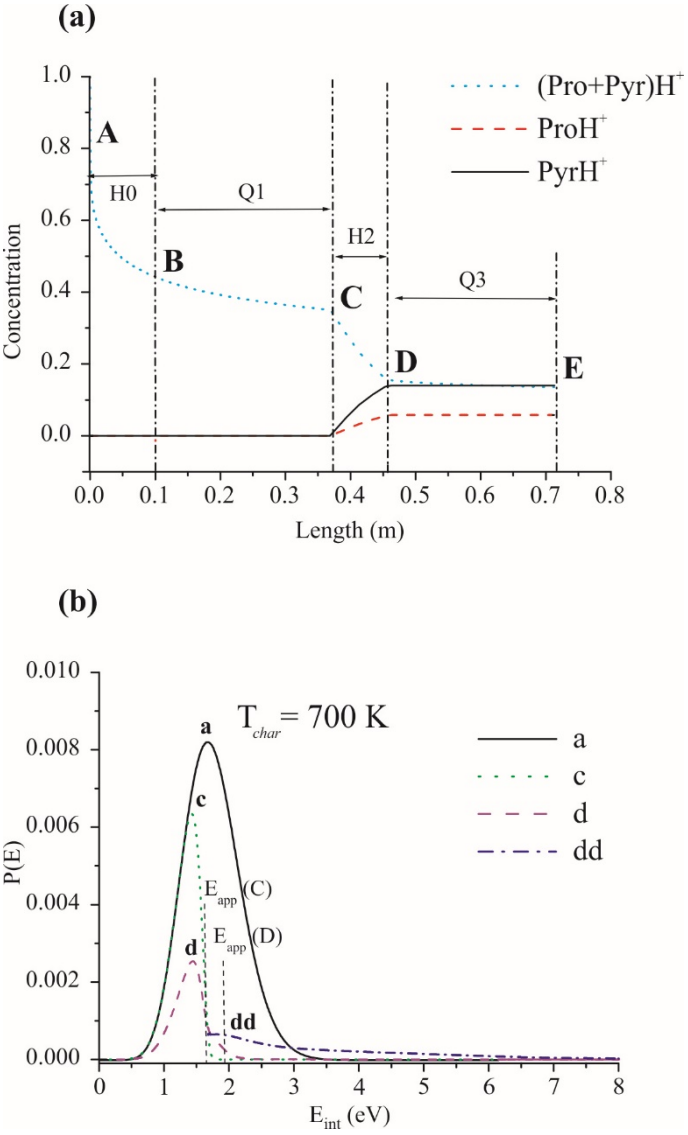

Figure S1. Protonated proline-pyridine heterodimer (m/z 195) decomposition studies (MS and MS^2 modes). The proposed curves are calculated for a cone voltage of V_c = 10 V (T_{char} = 700 K), a collision energy E_{lab} = 30 eV and a mean number of 1.1 collisions. (a) Calculated concentrations of precursor and product ions *versus* flight length of the mass spectrometer. (b) Internal energy distributions of the precursor ion calculated at different point of the mass spectrometer 'a', 'c', 'd' at point A, C, D respectively and 'dd' is the resulting "*hypothetical*" curve of collisional activation if no decomposition occurs into the gas cell using argon as collision gas). The maximum energy transferred during one collision is reported as E_{CM}. Note that multiple collisions of the precursor ion are unexpected. The area of 'a' is normalized to 1.

It was shown that the internal energy distribution of ions produced by an electrospray source can be well approximated by a thermal-like Boltzmann distribution and therefore, can be characterized by a temperature. This temperature is often called the characteristic temperature (T_{char}). For the proposed example this temperature is set equal to 700 K (curve 'a' (Fig. S1(b)).

In the H0 transfer hexapole, no more activation takes place. Thus, the concentration of the precursor ion decreases, leading to the two competitive product ions, $ProH^+$ and $PyrH^+$. After H0, the precursor heterodimer ion continues to decompose into the quadrupole mass filter Q1. The product ions formed into Q1 are lost. The internal energy distribution 'c' is related to the survival precursor ion that should be detected at detector 1, placed at the end of the first quadrupole analyzer Q1 (flight length = 0.358 m, point C). The corresponding area observed under the curve 'c' is the calculated precursor ion abundance.

The survival protonated heterodimer is mass selected by the Q1 analyzer for MS^2 experiments. In the RF only hexapole collision cell (H2), this ion is accelerated to perform collisions with the target argon gas. During the collisional process, a fraction of the kinetic energy of the ion is converted into internal energy. The extent of fragmentation depends on the new internal energy of the re-excited ion. The curve 'd' (Fig. S1(b)) is the internal energy distribution of the precursor ion calculated after the collision cell H2 using argon as target gas. A "hypothetic distribution", corresponding to the collision activation of the survival precursor ions where no decomposition in the gas cell is considered, is called curve 'dd'. However, for the precursor ions, multiple-collision processes are unexpected because a large part is decomposed after the first collision. So, the maximum energy transferred is related to the center of mass energy $E_{CM} = m_{Ar}/(m_{Ar}+m_{ion})E_{lab}$ which corresponds to an increase of 5eV for [Pro H+ Pyr] heterodimer and 30V collision energy. As a consequence, the area defined between the curves 'dd' and 'd' is equal to the sum of the abundances of product ions formed in the collision gas cell.

Effect of the thermokinetic parameters

Modification of the four major parameters: (1) the difference of critical energies (ΔE_0), which is related to the difference of proton affinities (ΔPA), (2) the difference of activation entropy ($\Delta\Delta S^{\ddagger}_{avg}$), (3) the initial value used for the critical energy (E_0), (4) the initial value used for the activation entropy ($\Delta S^{\ddagger}$) are proposed respectively in Fig. S2(a), (b), (c) and (d).

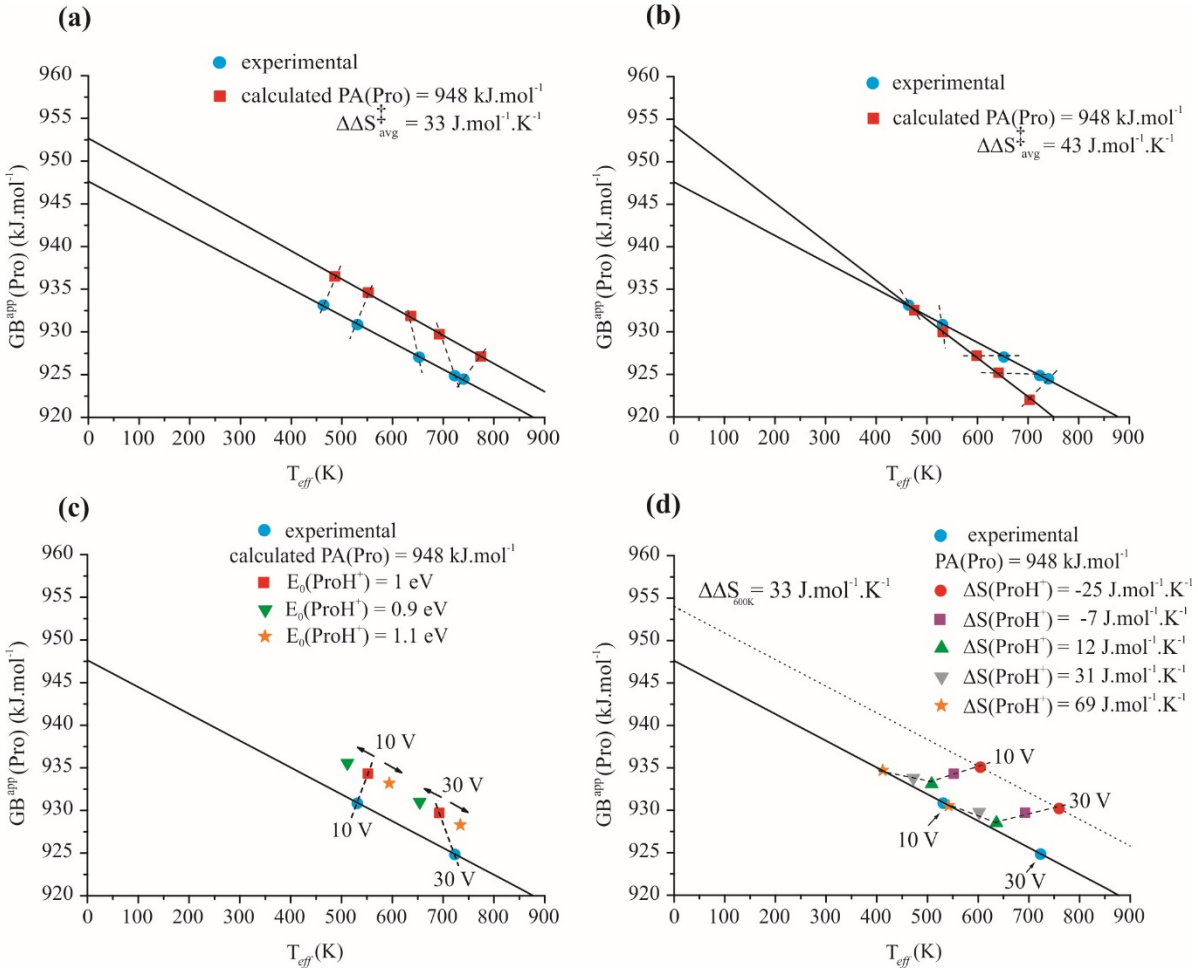

Figure S2. Experimental plot of "GB^{app}(Pro) vs. T_{eff}" and calculated curves using *MassKinetics* software (parameters in Table 1 are used for the calculations, except for PA(Pro), which is chosen equal to the experimental value PA(Pro) = 948 kJ.mol^{-1} and for the following parameters: (a) $\Delta\Delta S^{\ddagger}_{avg}$ = 33 J.mol^{-1}.K^{-1} (b) $\Delta\Delta S^{\ddagger}_{avg}$ = 43 J.mol^{-1}.K^{-1}; [$\Delta\Delta H_{298K}$ - $\Delta\Delta H_{0K}$] = 4.6 kJ.mol^{-1} (c) (■) $E_0(ProH^+)$ = 1 eV; (▼) $E_0(ProH^+)$ = 0.9 eV; (✶) $E_0(ProH^+)$ = 1.1 eV (d) (●) $\Delta S^{\ddagger}(ProH^+)$ = -25 J.mol^{-1}.K^{-1} ; [$\Delta\Delta H_{298K}$ - $\Delta\Delta H_{0K}$] = 2.8 kJ.mol^{-1} (■) $\Delta S^{\ddagger}(ProH^+)$ = -7 J.mol^{-1}.K^{-1}; [$\Delta\Delta H_{298K}$ - $\Delta\Delta H_{0K}$] = 3.5 kJ.mol^{-1}; (▲) $\Delta S^{\ddagger}(ProH^+)$ = 12 J.mol^{-1}.K^{-1}; [$\Delta\Delta H_{298K}$ - $\Delta\Delta H_{0K}$] = 3.4 kJ.mol^{-1} (▼) $\Delta S^{\ddagger}(ProH^+)$ = 31 J.mol^{-1}.K^{-1}; [$\Delta\Delta H_{298K}$ - $\Delta\Delta H_{0K}$] = 2.8 kJ.mol^{-1} (✶) $\Delta S^{\ddagger}(ProH^+)$ = 69 J.mol^{-1}.K^{-1} [$\Delta\Delta H_{298K}$ - $\Delta\Delta H_{0K}$] = 1.4 kJ.mol^{-1}.

1) The modification of the difference of critical energies (ΔE_0) is made by the change of the difference of proton affinities (ΔPA); the $E_0(ProH^+)$ = 1.0 eV is unchanged (Fig. S2(a)). The use of PA(Pro) = 948 kJ.mol^{-1} (instead of 944.5 kJ.mol^{-1}), which is the experimental value measured by alternative methods, leads to inaccurate simulations and a shift of around 4 kJ.mol^{-1} for the calculated curve is observed.

(2) The modification of the difference of activation entropy ($\Delta\Delta S^{\ddagger}_{avg}$) is made by the modification of the $\Delta S^{\ddagger}(B_iH^+)$ value ; the $\Delta S^{\ddagger}(ProH^+)$ = -7 J.mol^{-1}.K^{-1} is unchanged. For the proposed example the $\Delta\Delta S^{\ddagger}_{avg}$(600 K) is equal to 43 J.mol^{-1}.K^{-1} (values used in *MassKinetics*

software). The simulations are also made using the experimental PA(Pro) = 948 kJ.mol^{-1} (Fig. S2). From the slope of the calculated curve, the $\Delta\Delta S^{\ddagger}_{avg}$ is measured equal to 45 J.mol^{-1}.K^{-1}. This value is close to the fixed value used for calculations (43 J.mol^{-1}.K^{-1}). Nevertheless, the PA value (Y-intercept for 0 K) is measured 6 kJ.mol^{-1} higher than the value used in the software. As a conclusion, for all cases studied, the use of a $\Delta\Delta S^{\ddagger}_{avg}$ value different from 33 J.mol^{-1}.K^{-1} does not allow to fit experimental results.

(3) The modification of the initial value used for the critical energy (E_0) does not lead to significant change of the calculated curves. For the curves proposed Fig. S2(c), $E_0(ProH^+)$ is equal to 0.9 eV or 1.1 eV (instead of 1.0 eV) and ΔE_0 is unchanged. The lowest E_0 value leads to a shift of the "GB^{app}(Pro) vs. T_{eff}" curves to lower effective temperatures. Nevertheless, from the calculated curves, the PA(Pro) and $\Delta\Delta S^{\ddagger}_{avg}$ set values measured using the Armentrout's alternative method are unchanged.

(4) The effect of the initial value used for the activation entropy ($\Delta S^{\ddagger}$) is proposed Fig. S2(d). Modifications of $\Delta S^{\ddagger}(ProH^+)$ and $\Delta S^{\ddagger}(B_iH^+)$ are made by the change of the pre-exponential factors used in *MassKinetics* software ; the $\Delta\Delta S^{\ddagger}_{avg}$(600 K) = 33 J.mol^{-1}.K^{-1} is unchanged. The modification of $\Delta S^{\ddagger}(ProH^+)$ value leads to no change of $\Delta\Delta S^{\ddagger}_{avg}$ and small change of PA(Pro) values measured from the calculated curves (slops and Y-intercept to 0 K of the calculated curves, respectively). However, a modification of the calculated effective temperature is observed. Note that for convenience, only two points (10 V and 30 V) are reported Fig. S2(d). Nevertheless, as previously mentioned in Fig. S2(a), the calculation of six points (1 V to 50 V) shows the non-linearity of the curves "GB^{app} vs. T_{eff}" especially for the loose transition states (R^2 = 0.9918, 0.9965, 0.9983 and 0.9994 for $\Delta S^{\ddagger}(ProH^+)$ = -25, -7, 12 and 31 J.mol^{-1}.K^{-1}, respectively; results not shown).

Collisional efficiency and average number of collisions.

As proposed Fig. S3(a), an increase by a factor of five of the average number of collisions leads to no effect on the calculated curve "GB^{app} *vs*. T_{eff}". A poor effect is observed for a decrease by a factor of ten. Note that the real average number of collisions may be closely estimated from SY_E measurements (experimental SY_E = 0.46 at 30 V collision voltage for [Pyr H^+Pro]).

The effect of the collisional efficiency value used is proposed Fig. S3(b). The change of collisional efficiency to 0.15 instead of 0.3 leads to a shift of the "GB^{app}(Pro) *vs.* T_{eff}" curves to lower effective temperatures. Nevertheless, it is important to note that the GB^{app}(Pro) and

$\Delta\Delta S^{\ddagger}_{avg}$ set values measured from the calculated curves using the Armentrout's alternative method are unchanged.

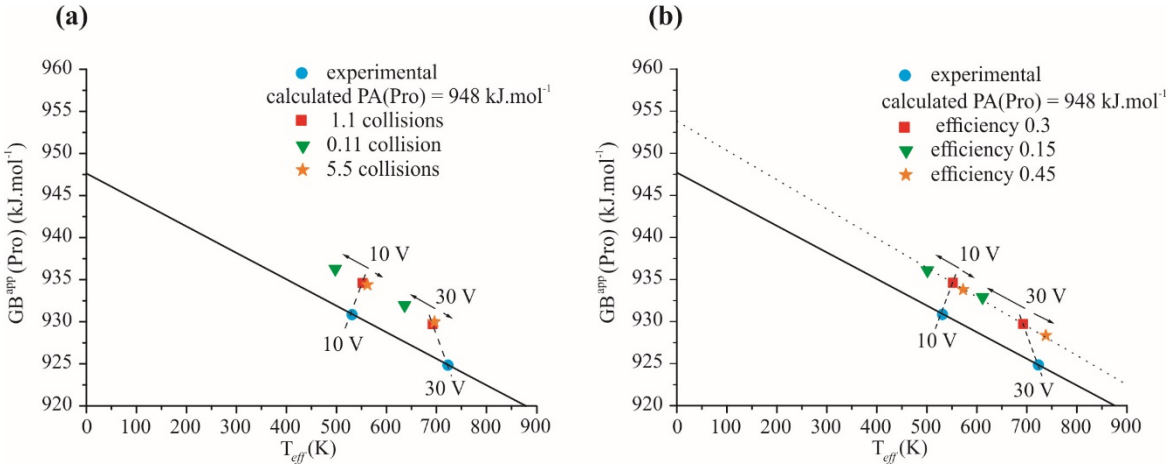

Figure S3. Experimental plot of "GB^{app}(Pro) vs. T_{eff}" and calculated curves using *MassKinetics* software (parameters in Table 1 are used for the calculations, except for PA(Pro), which is chosen equal to the experimental value PA(Pro) = 948 kJ.mol^{-1} and for the following parameters: (a) average number of collisions (■) 1.1 (▼) 0.11 (✶) 5.5 (b) efficiency of collision (■) 0.3 (▼) 0.15 (✶) 0.45.